CHAPTER 184

WAVES AND CURRENTS AT THE EBRO DELTA SURF ZONE: MEASUREMENTS AND MODELLING

Rodriguez,A.; Sánchez-Arcilla,A.; Collado,F.R.;
Gracia, V. Coussirat M.G. and Prieto J. [1]

Abstract

The wave incidence and the wave-induced circulation in the surf zone (SZ) is studied from both experimental and numerical point of view. The *DELTA'93* experiments were carried out in the Trabucador bar of the Ebro Delta, in the Spanish mediterranean coast. The emphasis of *DELTA'93* was on the SZ vertical flow structure, measuring simultaneously undertow and longshore current in a barred profile. The numerical simulation with *NEARCIR* Q3D model assumes longshore uniformity and stationarity. The wave decay, 2DH currents and 1DV undertow and longshore currents are modelled. The agreement is quite reasonable as can be seen in the included figures.

Introduction

The Ebro delta, one of largest in the Mediterranean, is located on the Spanish coast, 200 Km Southwest of Barcelona (figure 1). As in many other deltas of the world, the Ebro delta is experiencing a severe erosion due to the nearly total reduction of solid river discharges associated to dam construction (Jimenez and S.-Arcilla, 1993). Because of this there is an important monitoring activity around the deltaic coastline from which hydrodynamic, morphodynamic and meteorological data have been extracted to support the surf-zone campaign, which is the main object of this paper.

The data recorded during the surf-zone campaign, which took place along the Trabucador bar, will be described in this paper, together with some references to the wealth of previously recorded information along the deltaic coastline. The numerical model used to simulate surf-zone processes and to gain insight into the physics at the Ebro delta surf-zone during the time of the campaign, is the NEARCIR model presented in (S.-Arcilla et al., 1990/1992). This Q3D model works at the current time-scale and is structured into three modules:

[1] Lab. Ing. Marítima , L.I.M., Univ. Politécnica de Cataluña, U.P.C. Av. Gran Capitán s/n, 08034 Barcelona, Spain.

i. Wave Propagation Module (based on the kinematic conservation principle and the wave action balance equation).

ii. Depth Uniform Current Module (based on the 2DH rigid-lid mass and momentum equations).

iii. Depth Varying Current Module, including the Bottom Boundary Layer (this module is briefly described for completeness within this paper).

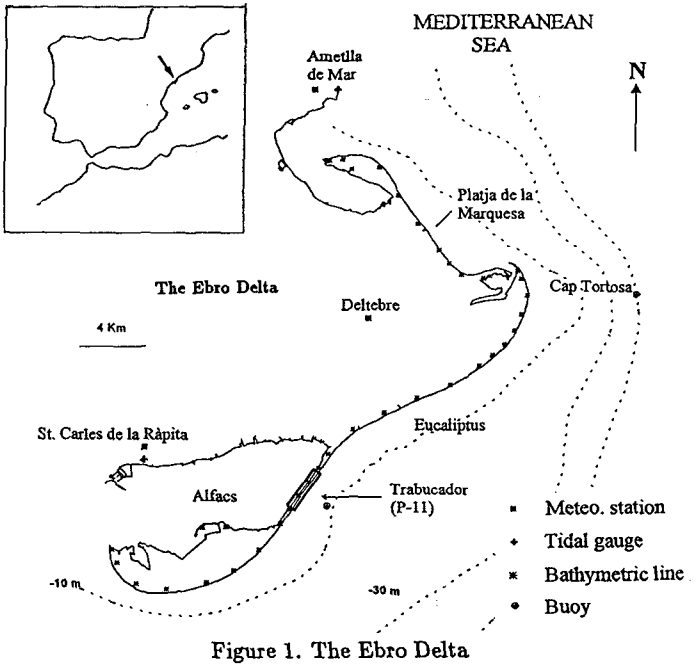

Figure 1. The Ebro Delta

DELTA'93 Field Experiments

The motivation for this campaign was the lack of detailed 3D data on surf-zone hydrodynamics in a microtidal environment. The campaign was thus focussed on the 3D structure of wave-induced circulation, i.e. on the simultaneous vertical structure of shore-normal (undertow) and shore-parallel (longshore current) flows. Because of this, and trying to avoid excessive complexities and/or unknowns, it was decided to look for an alongshore uniform beach subject to unidirectional waves and a time interval without significant wind.

Based on these considerations and because of the availability of previously recorded field data, the Trabucador bar in the Ebro delta was selected as the most suitable coastal stretch to carry out the surf-zone field exercise. The campaign was centered around the beach profile P11 (see figure 1). The obtained field data include bathymetry, shoreline, wave data outside and inside the SZ, mean water levels across the SZ, and the associated velocity fields (both

horizontal and vertical structure).

The bathymetry in the field site is shown in figure 2. Only relatively modest bottom variations were recorded during the three days of the campaign, which allows assuming a steady bottom geometry for the hydrodynamic analyses. The wave climate was recorded at 50 m and 7.5 m water depth by means of two directional wave rider buoys recording 20 minutes every 3 hours. An Etrometa step wave-gauge was located at the beach sledge, which was used to monitor hydro- and morphodynamic conditions across the surf-zone from the shoreline down to 2.5 m water depth. A BW video camera, placed at 20 m height, was used to record SZ images from which, after digital image processing, information on wave direction, breaking intensity, etc. could be obtained. An X-band radar was also used to measure mean surface roughness (mean wave height) and low-frequency oscilations of the mean water level in the SZ and adjacent nearshore area.

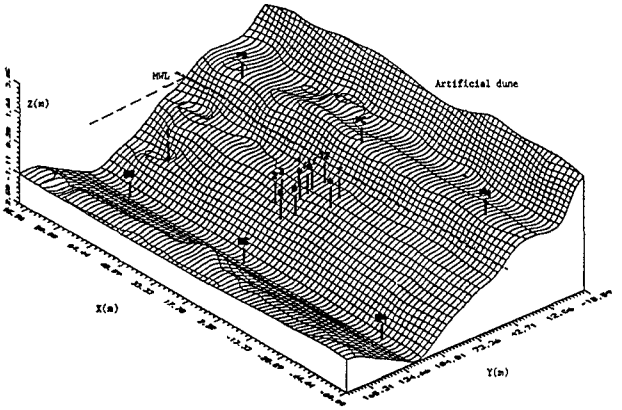

Figure 2. The Trabucador bar bathymetry (P11) for 16/December/93.

Some wave field characteristics plus 2DH circulation and mixing patterns derived from the video images using the developed digital processing technique have been presented in Redondo et al. (1994). This technique allows to quantify the time and space evolution of sea surface tracers (foam, dyes and Lagrangian buoys) and the horizontal mixing properties associated to dye spots.

The vertical structure of horizontal instantaneous velocities was measured with six electromagnetic current meters (Delft Hydraulics-S type) placed in a vertical pole at the sledge, see figura 3. The vertical spacing of the electromagnetic sensors (ems) range from 0.10 to 0.20 m above the bottom up to maximum level of 0.80 m above the bottom, with a sampling rate of 20 Hz allowing therefore to measure some macroturbulence features. Simultaneously with the velocities, the local water level evolution was measured at the same vertical with the step wave-gauge mentioned above (sampling rate 4 Hz). The MWL was computed by averaging the free surface time series, while crest and trough

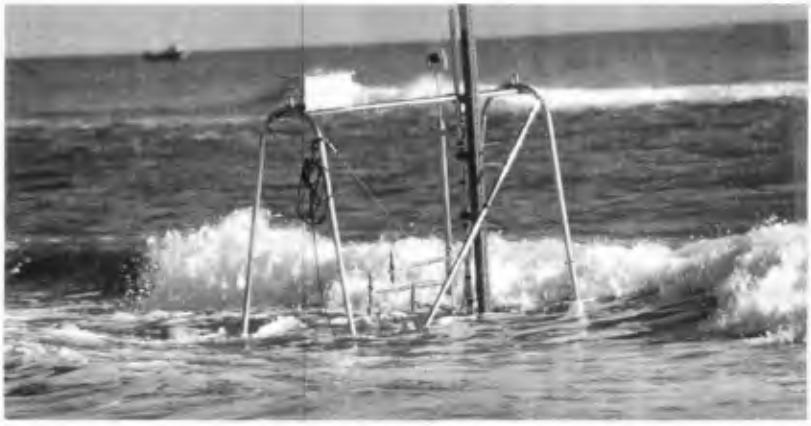

Figure 3. Movable Sledge with: 6 EMS, 1 WG, 3 OBS, 1 COMPASS, Data-Logger and 1 Optic-Prism).

levels were obtained as the mean of the upper "1/3" series of individual crest and trough values. The crests and troughs were obtained after numerically filtering the original water-surface series to remove the effect of long waves and other alien-phenomena.

Waves: Measurements and Modelling

Wave Features

Table 1 summarizes the 5 cases measured during the *DELTA'93* experiments.

Cases	Date	I. E. L.	Spectra	T_p (s)	Sea State	Test n.
I	26/05/93	High	doubled-peak	T_{p1} 18 T_{p2} 3	unsteady	-
II	15/12/93	Low	wide	7.5	Q-staedy	NT1-NT4
III	16/12/93 a.m.	Medium-High	sharp	6.0	Q-steady	NT5-NT7
IV	16/12/93 p.m.	Medium	sharp	5.5-7.0	unsteady	NT8-NT12
V	17/12/93	Low	wide	7.5	steady	-

Table 1: Measured conditions I.E.L.: Incident wave energy level; Spectra: type of wave spectra; T_p: wave period; Test n.: Test number

In this paper only cases III and IV, measured during 16th December 1993, are considered for an in-depth analysis because they were the most complete cases with strong enough wave-induced currents. There are several potencial sources of error, such as the linear interpolation in directional wave data recorded every

3 hours by the buoy (to have time correspondance with the wave gauge data recorded every half-hour), the spreading in wave direction given by the buoy or those inherent to the measurement equipment and processing techniques. In spite of this, there was reasonable agreement between the surf-zone spectra from wave-gauge and video images data, showing a good correspondance of frequencies or dominant periods. The comparison between wave angles from the video (VTR) and the ems is not finished because of the large amount of data-processing necessary to obtain a mean angle of wave incidence. The incident wave conditions during the 16th December 1993 (outside and inside the SZ) are sumarized in tables 2 and 3. Hrms (m) is the root mean square wave height, Tp(s) is the wave period, θ_m is the mean angle of wave incidence, X is the crosshore coordinate, h is the mean water depth and U-V (m/s) are the depth-averaged cross- and alongshore velocity components at different sledge positions (test) inside the surf-zone.

Wave incident conditions (DWR)				
Test	Hrms (m)	Tp(s)	θ_m	GMT
5	.61	6.0	177.0	10:04
6	.60	6.1	175.3	10:55
7	.59	6.3	173.0	12:05
8	.50	5.7	179.5	14:07
9	.44	5.4	183.3	15:07
10	.43	5.4	180.6	15:46
11	.425	5.6	176.1	16:20
12	.42	5.8	171.9	16:51

Table 2: Incident wave conditions at *dwr* position (1500 m offshore, h:7.5m) during 16/December/93.

Hydrodynamic measurements in the SZ						
Test	Hrms	Tp(s)	X(m)	h(m)	V^*	U^*
5	.47	7.1	87.9	1.29	.48	.15
6	.38	7.1	73.2	0.80	.88	.19
7	.31	8	65.1	0.70	.66	.13
8	.41	7.1	93.5	1.34	.23	.08
9	.40	7.1	79.8	0.70	.62	.24
10	.33	7.1	74.0	0.68	.60	.16
11	.27	8	69.5	0.60	.46	.11
12	.18	8	60.0	0.38	.28	.10

* (mean below wave trough level z_{tr})

Table 3: Hydrodynamic conditions from WG and *ems*

An image processing technique, still under development, has also been used to evaluate the acrosshore distribution of the intensity of wave breaking, Q_b. From an image threshold intensity associated to breaking, the breaking wave distribution acrosshore can be determined for a time series of beach profile transects derived from the video record. The processing technique is able to reproduce some of the features of the acrosshore evolution of the fraction of breaking waves, as derived from e.g. the Battjes and Janssen (1978) (hereinafter

BJ'78) model (figure 4).

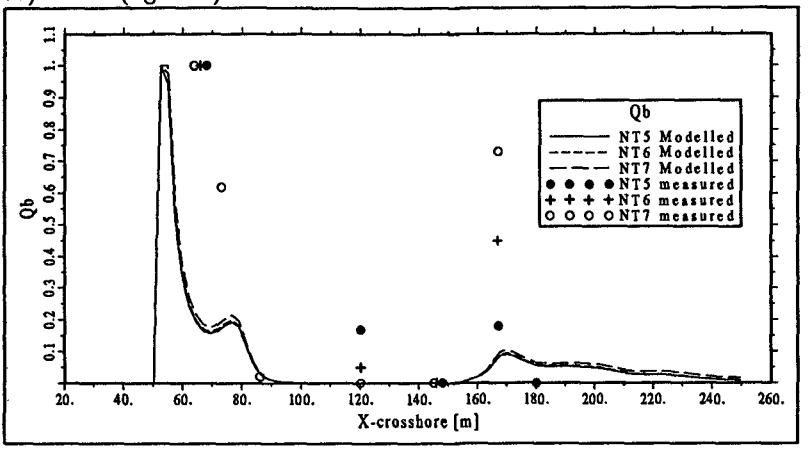

Figure 4. Measured and computed Qb for case III (around 100 waves)

Wave Propagation

The wave conditions for cases III and IV were quasi-stationary, although in this latter case a transient component was also apparent (see test 8 in figure 5). Wave decay due to breaking has been modelled using the BJ'78 approach for random waves (neglecting bottom disipation). In spite of the lack of perfect stationarity the obtained results are quite reasonable (figure 6). The single value used for the dissipation parameter α, leads to overestimating the higher wave values near the shore. Moreover, in this shoreline region, the shoaling process dominates over the breaking-induced decay which yields some oscillations in the cells of the computational domain close to the shoreline (not appreciable in figure 6).

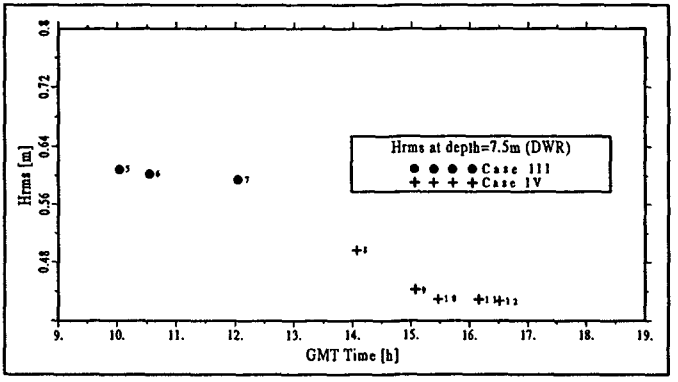

Figure 5. Wave height (Hrms) at 7.5 m depth from DWR

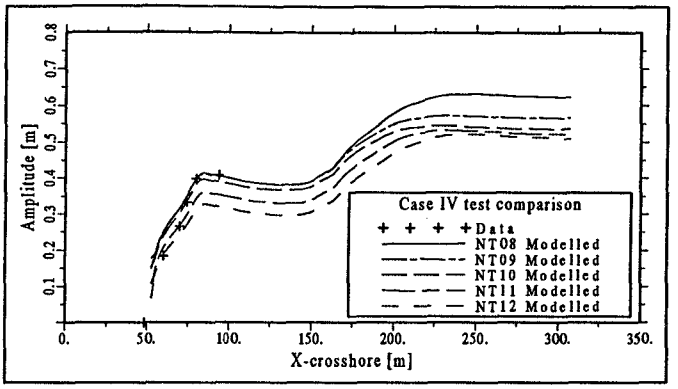

Figure 6. Wave decay Case IV. The different lines correspond to the varying conditions at the offshore boundary corresponding to the SZ-test time.

To achieve a reasonable setup prediction, a general sea level rise due to storm-surge has to be assumed in the field data. This general sea level rise has been estimated in 15cm and 8cm for cases III and IV respectively, using an iterative process. The resulting setdown/up predictions are reasonable although the fit is far from perfect. There is not yet a satisfactory explanation for this mean water level behaviour (figure 7). The predictions of the angle of wave incidence are in general acceptable (see figure 8), although numerical results overpredict systematically the experimental data from the ems. The origins for this could be the procedure used to derive an angle of wave incidence from the ems data, the spreading in wave angle given by the directional buoy (which is quite high when compared to the accuracy of the computations) or wave current interaction effects which have not been considered in this preliminary analysis.

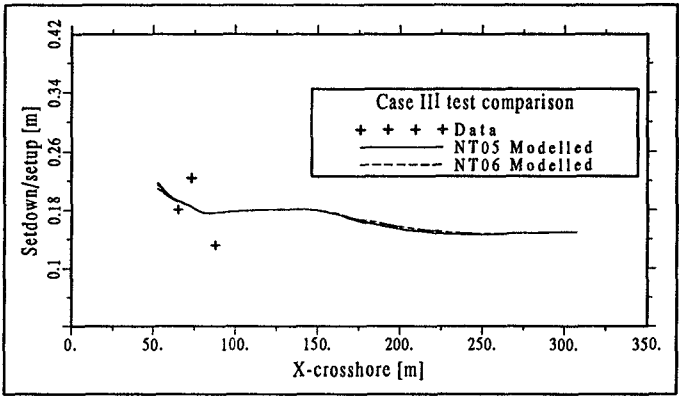

Figure 7. Wave setdown/setup for Case III.

Apart from the incident wind waves, there was evidence of stationary long waves with a period of around 40 s in the water surface time series. This long period pulsations are more clear in the spectral and moving average analysis of the velocity time series, both for the longshore and undertow components. These pulsations were uncoupled for longshore and cross-shore currents in most

of the measured tests. The longer period oscillations and the macroturbulence features are still being processed and will not be further discussed in this paper.

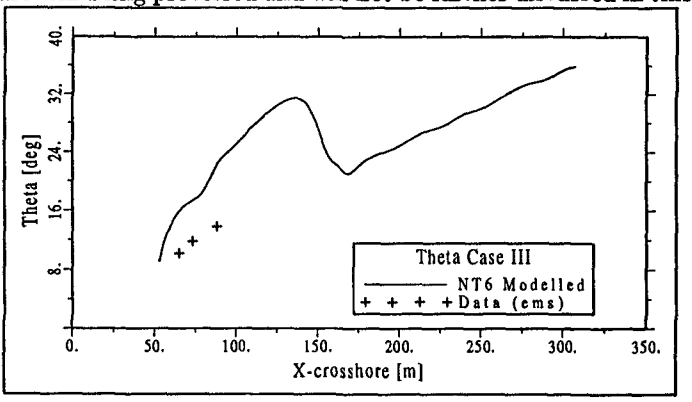

Figure 8. Incident wave angles for Test 6, Case III

The current measurements have shown the coexistence of a strong longshore current with a clear undertow crosshore distribution. The general pattern of measured data agree with the expected 3D "helicoidal" current structure shown in figure 9. Aditionally it was observed the maxima for cross- and longshore components located at roughly the same across-shore coordinate.

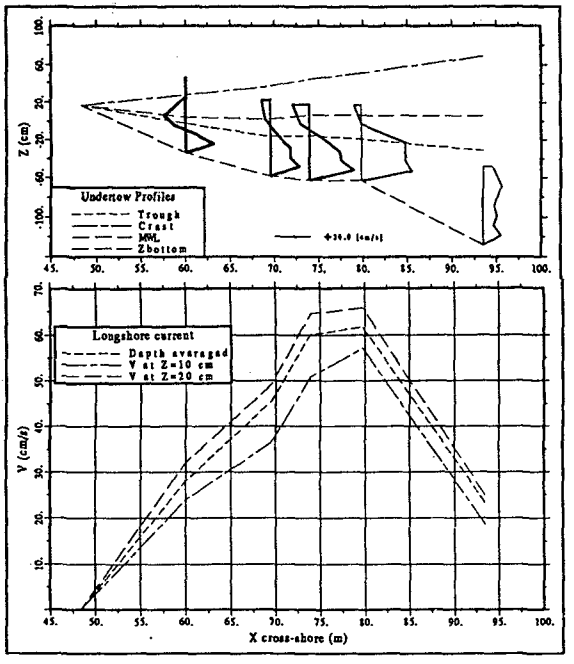

Figure 9. Measured 3D current field structure for Case *IV*.

Depth Averaged Currents

The velocity data were obtained after debbuging, compass-correction and quality controls applied to the "raw" time series. The mean (referring to time and depth average) current values were calculated after time and vertical averaging over the series length (from 20 to 40 minutes depending on the record) and from the bottom up to the highest sensor (always below trough level).

Eulerian (ems) and Lagrangian (buoys and dye-spots) current velocities have been compared for the same time and space intervals, showing reasonable agreement eventhough the potential sources of error are different for each type of measurements. The main sources of error include the dye-spot location in the vertical, inaccuracies of the pixel-coordinates transfer function, ditto for the ems-orientation, limitations of the scale range and those inherent to the processing/filtering technique.

The 2DH currents have been modelled assuming an alongshore uniform beach which implies a mass balance restriction per profile. The bottom shear stress is modelled using a standard linear expression and the horizontal eddy viscosity coefficient follows the De Vriend and Stive (1987) (hereinafter DVS'87) proposal. These values agree well with the experimental data obtained from the processing of dye dispersion images (see Rodriguez et al, 1995). The numerical domain extends up to the shoreline, considering dynamically the "dry-flood" problem in that region.

The obtained results are quite reasonable (see figure 10) with two maxima roughly in the region of the two bars present in the profile. The mean cross-shore flux, obtained using the external mass flux closure submodel of DVS'87, is acceptable only in some regions. This point must be clearly improved in the future, from which better longshore current predictions can be expected.

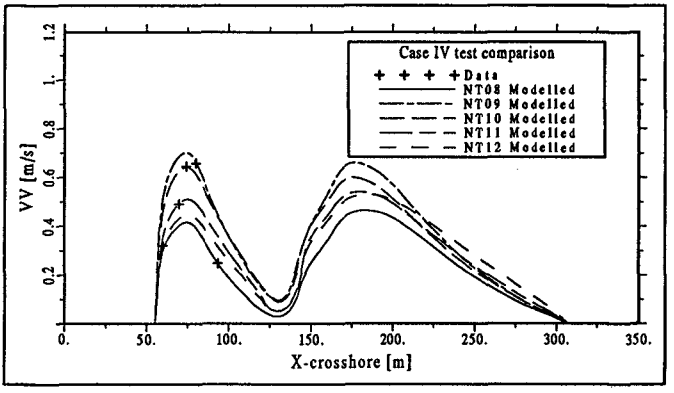

Figure 10. Longshore currents for Case IV. The different lines correspond to the hydrodynamics conditions of fig. 6.

1DV Structure of Currents

The vertical flow structure during *DELTA'93* was monitored with six ems

placed at 0.1, 0.2, 0.3, 0.4, 0.6 and 0.8 m above the bottom, at a single vertical pole located at the sledge. Measurements above z_{tr} were used to estimate the mass flux during the "wet intervals". Measurements below z_{tr} were used to characterize the vertical profiles of longshore and cross-shore currents, outside the bottom boundary layer (BBL).

The undertow profiles show a maximum near the bottom as expected according to previous experimental information (see e.g. Okayasu, 1989 or Smith et al., 1992). The longshore current profiles below z_{tr} show a mildly increasing trend upwards rather than a constant value.

The 1DV module, described in S.-Arcilla et al. (1992), splits the total current velocity vector into depth uniform, $\vec{\bar{u}}$, and depth varying, $\vec{\tilde{u}}$, components. The crest-to-trough layer is not solved because it is considered exclusively via its interaction with the middle layer at trough level through the imposition of the appropiate boundary conditions. The BBL model is inspired on the one proposed by Fredsøe (1984), whose solution leads to algebraic expressions of logarithmic form that have been here parameterized to achieve an economic solution. The middle layer equations are solved using a power series approximation, $\sum_1^N a_i z^i$, to reproduce the vertical variation of $\vec{\tilde{u}}$.

It can be shown theoretically (S.-Arcilla et al, 1992) that the middle layer equation may not converge under certain conditions. Because of that, in general, the profile obtained consists of a first logarithm within the BBL, from z_o up to z_b, $(z_b - z_o = \delta_m)$, a second one up to a given z_l level, and from this level to z_{tr} the power series $a_i z^i$.

The "optimal" z_l level to achieve an efficient convergence and to avoid artificial profile distorsions is here considered to be $z_l \simeq 0.2 z_{tr}$. The trough level z_{tr} has been estimated as:

$$z_{tr} = max\ [0.8h; h - 0.5H_{rms}]$$

The $\vec{\tilde{u}}$ model needs three main external closure submodels to determine the $\vec{\tilde{u}}$ profile: a) the shear stress $< \vec{\tau_{tr}} >$ at trough level, b) the mass flux over this level, $< \vec{Q_s} >$, and c) the eddy viscosity vertical distribution, $\nu_t(z)$.

For the case of longitudinal uniformity, the mean cross-shore velocity $\bar{u}$ is obtained using a Q_s expression similar to the one proposed in DVS'87. This expression, which is given by:

$$< Q_{sx} >= (1.0 + 7.0\ Q_b \frac{h}{L}) \frac{E}{\sigma} K_x$$

does not fit well the experimental $\bar{u}$ (see figure 11). In the $< Q_{sx} >$ formula Q_b is a measure of the breaking intensity, h is the water depth, L the wave length, E the wave energy density, σ the wave frequency and K_x the x component of the wave number vector.

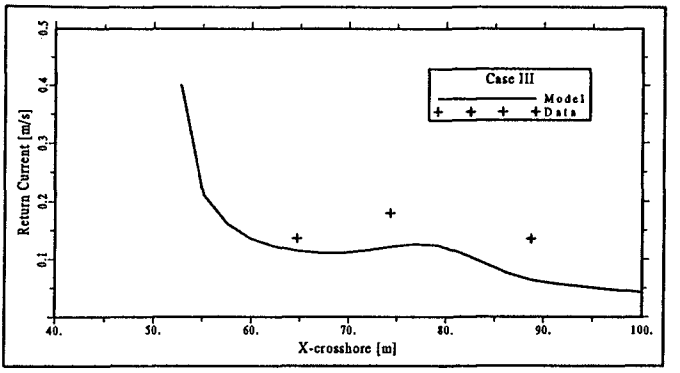

Figure 11. Crest-to-trough mass flux calculated according to DVS'87 and measured mean flow values (across-shore distribution)

The closure model for $< \vec{\tau_{tr}} >$ uses the general expression proposed by Deigaard (1993), which extends the 1-dimensional expression obtained in Deigaard and Fredsøe (1989). The closure model for the eddy viscosity allows either a constant or a parabolic form for ν_t. The resulting expression is made up of two terms, the first one corresponding to the current induced eddy viscosity (similar to the one proposed in e.g. Coffey and Nielsen (1984)) and the second one corresponding to the breaking induced eddy viscosity similar to the value proposed by DVS'87 and Battjes (1983).

The resulting undertow profiles for cases III and IV are obtained with a constant ν_t and $N = 20$ in the middle layer equations, see figures 12 and 13. The continuous line represents the modelled undertow using as mean return flow the experimental value, while the dashed line represents the modelled undertow with an analytically calculated mean mass flux. It is apparent that the model fits much better the measured vertical structure when the experimental mean mass flux is used. The obtained fit is quite satisfactory eventhough there are no data from the bottom boundary layer.

The values above trough level, also indicated in the figures, have only been used to calculate the mean mass flux. Points I and II, physically "unrealistic", have been disregarded. No explanation for these two points is available. It can be, thus, concluded that most of the profiles show a good agreement between experimental and modeled values in the middle layer. This agreement is also reasonable near the bottom, although there is a small trend to understimate measured current values in the lower part of the water column.

The corresponding longshore current vertical profiles for cases III and IV are shown in figures 14 and 15. The model results, which are preliminary, have been obtained using a parabolic power series. The solution with the complete power series is now been tested although the fit appears to be reasonable enough with the second order approach.

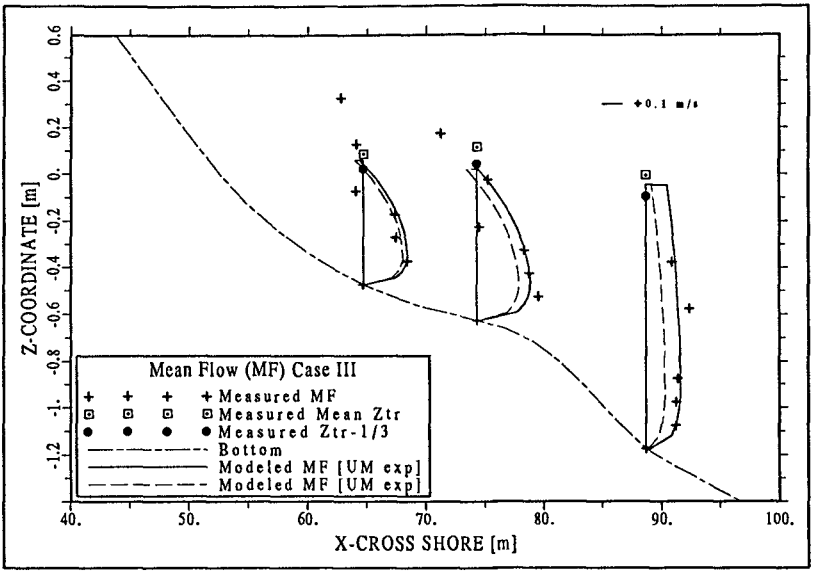

Figure 12. Undertow measured and modeled for Case III.

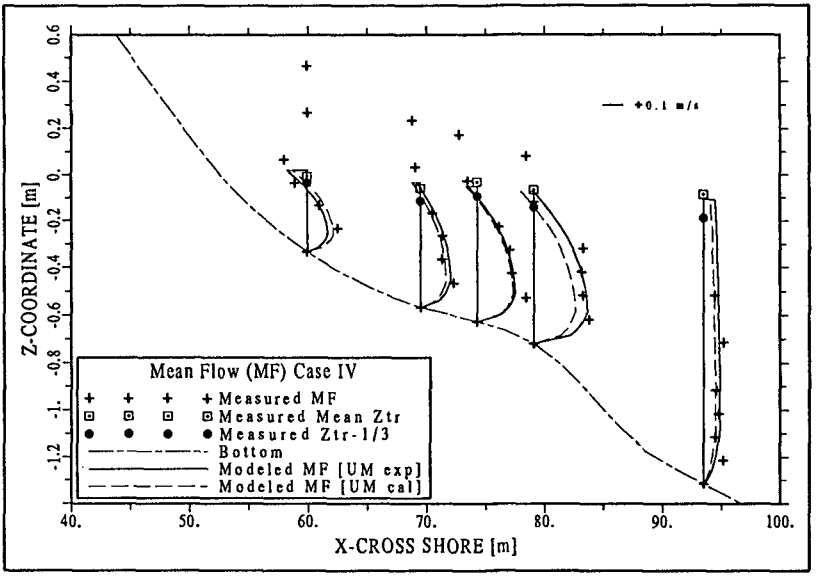

Figure 13. Undertow measured and modeled for Case IV.

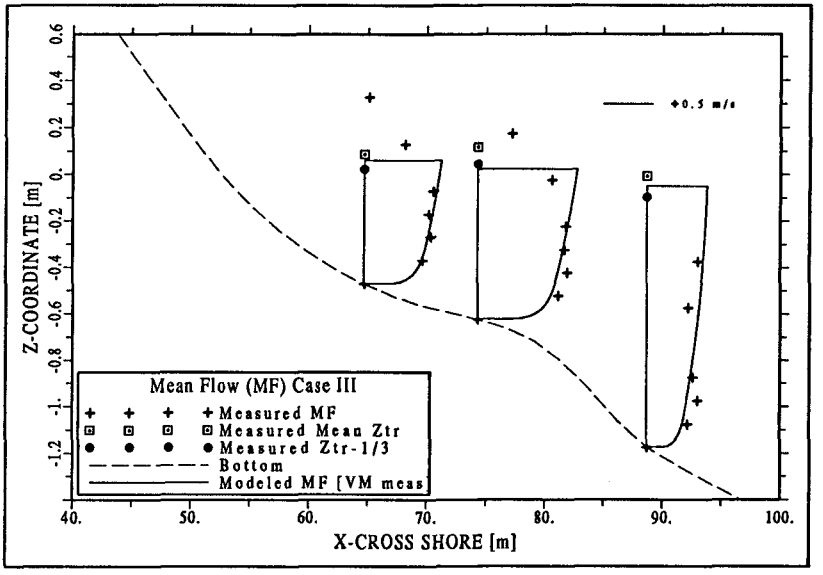

Figure 14.Longshore currents measured and modeled for Case III, (note rotated longshore profiles from the $z-y$ to the $z-x$ plane).

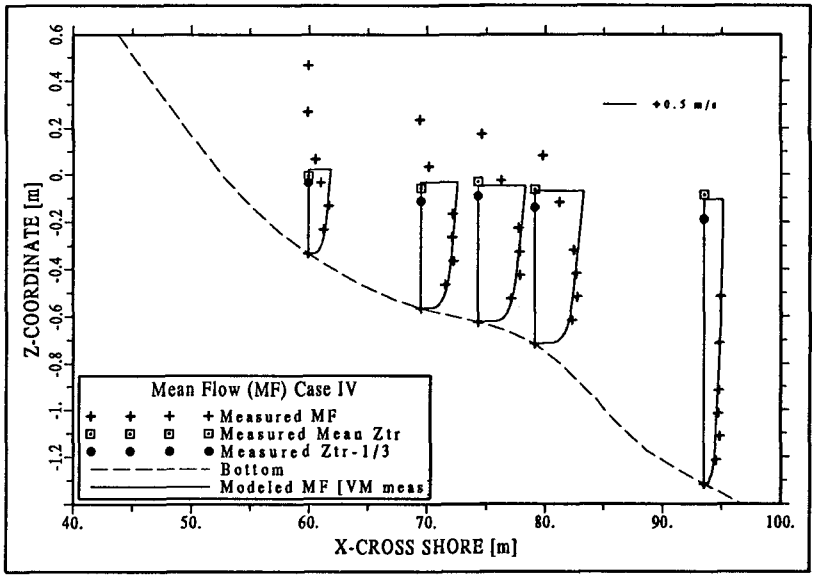

Figure 15.Longshore currents measured and modeled for Case IV.

Final Remarks

The *DELTA'93* field campaign is a modest field effort with respect to other experimental studies (e.g. DUCK, SUPERDUCK, NSTS, B-BAND, EGMOND, C2S2, NERC, DELILAH, etc.). The emphasis of *DELTA'93* was on the SZ vertical flow structure since the Mediterranean sea is an adequate environment to study this kind of processes, due to its microtidal range and medium wave energy-level characteristics.

The developed methodology works successfully eventhough there were some difficulties to define what was the still water level and what was the mean water level due to setup, setdown and storm surge. The identification of different flow modes (e.g. splitting up between low frequency, high frequency and current type motions) needs to be careful due to the non-negligible dependence on the filtering/processing techniques.

Long period pulsations are clear in the spectral analysis of the velocity time series, both for the longshore and undertow components. These pulsations were uncoupled for longshore and cross-shore currents in most of the tests.

The general pattern of measured data in the SZ agree with the expected 3D "helicoidal" current structure (figure 9). The maxima for cross- and longshore components happen at roughly the same across-shore coordinate.

The undertow profiles show a maximum near the bottom and the longshore current profiles below z_{tr} show a mildly increasing trend upwards rather than a constant value.

A good estimation of Q_b from video images needs time series longer than 100 waves period.

The disipation model have showed difficulties in the fitting of the measured data when it was applied in the considered domain.

With respect to the modelling effort a general conclusion is the inherent limitation of field data to accurately validate numerical models. These numerical models always simulate a much simplified situation with respect to the field one, which precludes any definite and accurate validation conclusions for the time being.

In the wave modelling part there were in general good agreement with a slight overpredicted wave heigts and some decay/shoaling oscillations near the shoreline. The main trouble with respect to the depth-averaged current modelling were the current overpredictions near the shoreline because of the decay oscillations just mentioned.

The 1DV model showed a good enough fitting of the vertical profiles, although the mass flux submodel should be improved due to its sistematic underpredictions. It was also noted a slight trend to underestimate the current values near the bottom.

Acknowledgements

This work was undertaken as part of the Surf Zone Research project of LIM-UPC. It was funded jointly by the Programa de Clima Marítimo PCM-MOPTMA and the Ministerio de E. y C. (DGICYT) of Spain, with some support from the MAST-II G8M Project of the E.U. We want to thank the research staff of LIM-UPC, particularly J Gomez , J Sospedra and all those who endured the field work. Thanks are also due to G Voulgaris and MA Tenorio from Southampton University for their OBS and radar; and to MJF Stive and JM Redondo for their helpful collaboration "before, during and after" the experiments.

References

Battjes J. (1983) Surf zone turbulence.*Proc. 20th IAHR Cong.*, Moscow.

Battjes J. and Jansen J. (1978) Energy loss and set-up due to breaking of random waves. *Proc. ICCE*, ASCE, pp 569-587.

Coffey F. and Nielsen P. (1984) Aspects of Wave Current Boundary Layer Flows.*Proc. ICCE*, ASCE, pp 2232-2245.

Deigaard R. and Fredsøe J. (1989) Shear stress distribution in disspative water waves.*Coastal Engineering*, 13, pp. 357-378.

Deigaard R. (1993) A note on the three dimensional shear stress distribution in a surf zone. *Coastal Engineering*, 20 , pp. 157-171.

De Vriend H. and Stive M.J.F. (1987) Quasi–3D modelling of nearshore currents. *Coastal Engineering*, 11, pp 565-601.

Fredsøe J. (1984) The turbulent boundary layer in Wave-Current Motion, *J.H.E*, ASCE, Vol 110, N^o 8, pp 1103-1120.

Jiménez J. and Sánchez-Arcilla A. (1993) Medium-term coastal response at the Ebro delta, Spain. *Marine Geology*, 114, pp. 105-118. Okayasu A. (1989) Characteristics of turbulence structure and undertow in the surf zone. Ph.D. thesis, University of Tokio, Japan.

Redondo J., Rodriguez A., Bahía E., Falqués A., Gracia V., Sánchez-Arcilla A. and Stive M.J.F. (1994). Image Analysis of Surf-Zone Hydrodynamics. *Proc. Coastal Dynamics 94*, ASCE, pp. 350-365.

Rodriguez A., Sánchez-Arcilla A., Redondo J., Bahía E., and Sierra, J.P. (1995), Pollutant dispersion in the nearshore region: modelling and measurements. *Int.Jour.Water Sc. and Tech.*, IAWQ, (in press).

Sánchez-Arcilla A., Collado F., Lemos C. and Rivero F. (1990) Another quasi-3D model for surf-zone Flows.*Proc. ICCE*, ASCE, Delft, pp. 316-329.

Sánchez-Arcilla A., Collado F. and Rodriguez A. (1992) Vertically varying velocity field in Q3D nearshore circulation. *Proc. ICCE*, ASCE, Venice, pp. 2811-2824.

Smith J.M., Svendsen I. and Putrevu, U. (1992) Vertical structure of the nearshore current at Delilah: measured and modeled. *Proc. ICCE*, ASCE, Venice, pp. 2825-2838.